Cement and Concrete Research 39 (2009) 1164–1173

Contents lists available at ScienceDirect

Cement and Concrete Research

journal homepage: http://ees.elsevier.com/CEMCON/default.asp

Early hydration of clinker–slag–metakaolin combination in steam curing conditions, relation with mechanical properties

F. Cassagnabère [a,b,*], M. Mouret [a], G. Escadeillas [a]

[a] Université de Toulouse, UPS, INSA; LMDC (Laboratoire Matériaux et Durabilité des Constructions), 135, Avenue de Rangueil; F-31 077 Toulouse Cedex 04, France
[b] SEAC-Gf, 47 Boulevard de Suisse 31 021 Toulouse, France

ARTICLE INFO

Article history:
Received 26 January 2009
Accepted 24 July 2009

Keywords:
Cement/slag/MK binder (D)
Steam curing (A)
Early age
Hydration product (B)

ABSTRACT

High strength can be obtained at early ages for precast concrete elements by the use of CEMI 52.5R cement (OPC) and thermal treatment (steam curing). To compensate for the announced withdrawal of CEM I cements because of high CO_2 emissions during their production and the ecotax that this will imply, one attractive alternative is the use of composed cements resulting from the combination of clinker with mineral admixtures. In steam curing conditions, previous studies have shown an increase in the compressive strength at one day of age for mortars incorporating an OPC/blast furnace slag (GGBS)/metakaolin (MK) combination, in comparison with mortars incorporating OPC only. The present study investigates the connection between the compressive strength, at one day of age, of steam cured mortars made with various binders and the hydration of these binders. The progress of the hydration was characterised by means of XRD, thermal and microprobe analyses. The results indicate that the increase in compressive strength when MK is incorporated (OPC/MK or OPC/MK/GGBS) can be explained by an increase in the amount of C-S-H, C-A-H, C-A-S-H phases, a decrease in the amount of CH and a change in the chemical nature of the matrix (decrease in *C/S* ratio). The decrease in compressive strength of OPC/slag-based material can be explained by a reduction in the amount of hydrated phases (particularly C-S-H) and compactness.
These are promising results for precast concrete manufacturers who are concerned about preserving the environment.

1. Introduction

At present, the precast industry is booming and represents 20% of concrete production worldwide [1]. Precasting is the production in a factory of either plain concrete elements (concrete masonry units, road kerbs, floor blocks, etc.) or reinforced/prestressed concrete elements (hollow core slabs, beams, underground arch stones, etc.).

The interest in precast products can be explained by the many advantages they offer, such as reductions in building time, the multiplicity of available products, assured quality with certified performance levels, optimised costs, etc. A major preoccupation for the precast industry concerns time delays because of their effect on profitability. To keep manufacturing times down, the concrete used to make structural precast beams and slabs must have good mechanical characteristics at both early and later ages. For instance, a high compressive strength as early as one day of age is required for prestressed concrete so that the pretensionned strands can be relaxed.

To achieve such mechanical properties, two solutions are recommended.

First, CEMI-52.5R cements (OPC) complying with European standard EN 197-1 [2] should be used because they combine high clinker content (at least 95% by weight, notation CEMI), high fineness (notation *R*), which enables high reactivity at an early age [3] and 28-day minimum compressive strength of 52.5 MPa (notation 52.5) measured on normalised mortars according to European Standard EN 196-1 [4].

Second, a high curing temperature (steam curing) should be employed to accelerate the maturation of precast products. It is widely reported that a high curing temperature favours the development of mechanical properties at early ages but can adversely affect the strength at later ages [5,6]. The through-solution mechanism is accelerated in the first stages of hydration by the rise in temperature. At later ages, the hydration reactions are essentially of a topochemical nature and, as such, take place mostly on the surface of the reacting materials. High curing temperature conditions rapidly increase the occurrence of topochemical reactions. Accordingly, an uneven distribution of the hydration products has an unfavourable influence on the strength of the whole material [7].

Combining these solutions (reactivity of CEMI 52.5R cement and acceleration of cement hydration kinetics by thermal treatment)

---

* Corresponding author. Université de Toulouse, UPS, INSA; LMDC (Laboratoire Matériaux et Durabilité des Constructions), 135, Avenue de Rangueil; F-31 077 Toulouse Cedex 04, France. Tel.: +33 5 61 55 67 11.
E-mail address: franck.cassagnabere@insa-toulouse.fr (F. Cassagnabère).

0008-8846/$ – see front matter © 2009 Elsevier Ltd. All rights reserved.
doi:10.1016/j.cemconres.2009.07.023

allows sufficient maturity to be reached at early ages for the prestressed elements to set in a tensile state.

However, due to the high clinker content, the production of CEMI 52.5R cement releases large amounts of CO2 into the atmosphere [8]. For example, during the decarbonation of raw materials, the alite phase (Ca3SiO5, i.e. C_3S) produces large quantities of CO2, as shown by the following basic equation (mass proportions in italics):

$$\begin{array}{cccc} 3CaCO_3 & +\ SiO_2 \xrightarrow{1350^\circ C} & Ca_3SiO_5\ + & 3CO_2 \\ 300 & 60 & 228 & 132 \\ \text{Calcium carbonate} & \text{Silica} & C_3S\,(\text{Alite}) & \text{Carbon dioxide} \end{array} \quad (1)$$

From Eq. (1), irrespective of the type and efficiency of the calcination process, every ton of C_3S produced releases 579 kg of CO2 and generates a minimum thermal energy of about 4.70 GJ at 20 °C. Moreover, the reaction cannot proceed at temperatures lower than about 1250 °C, even if a catalyst is used. In practice, it is necessary to bring the raw material temperature to 1400 °C so that the reaction rate is high enough to be cost-effective [9,10].

In such manufacturing conditions, the high CO_2 emission is becoming a matter of concern with regard to protection of the environment. The planned establishment of an ecotax means that CEMI cement could disappear in the near future [11].

To compensate for the increase in the consumption of CEM I cements [10], one attractive alternative is the use of compound cements resulting from the combination of clinker with mineral admixtures. However, the utilisation of such cements can become a realistic solution only if their raw constituents are present in the local market and if they do not affect the compressive strength in comparison with the CEMI cement that is currently used and gives satisfaction.

The authors [12] measured compressive strengths on steam cured mortars at early age (1 day). The composition of various mortars, named Mi, differed in the nature of the binder, named Bi (blended with the binder Bi = 450 g, Water/Bi = 0.5 and Sand/Bi = 3). They were made according to European Standard EN 196-1 [4]. Combinations of three raw materials were used to develop the binders: CEMI 52.5R cement, blast furnace slag (GGBS) and metakaolin (MK). Four binders could be derived from the different combinations.

- Primary binder B1 (100%CEMI 52.5R) defined as the reference binder.
- Secondary binders B2 (75%CEMI + 25%MK) and B3 (82%CEMI + 18%GGBS).
- Ternary binder B4 (61.5%CEMI + 13.5%GGBS + 25%MK).

In comparison with the compressive strength of the reference mortar M1 (33.9 MPa for CEMI only) at one day of age:

- the replacement of 25% of the mass of CEM I cement by MK (M2) generated a relative increase of 39%;
- the replacement of 18% of the mass of CEM I cement by GGBS (M3) led to a 19% decrease;
- the ternary binder B4 enabled a 31% increase.

The compressive strength data are gathered together in Appendix 1.

To try to explain these variations of strength when GGBS and/or MK partially replace cement in steam curing conditions, it would be interesting to investigate the hydration characteristics of the matrix.

Appendix 2 presents a review of fundamental studies dealing with the identification of hydrated phases existing at one day of age in materials that incorporate metakaolin or slag in high temperature curing.

- MK principally reacts with portlandite (CH) derived from cement hydration in the presence of water and generates hydrated phases identified as C-S-H gels chemically different from the ones derived from the hydration of plain cement, and neoformed phases like alumina-silicate hydrates C_2ASH_8 and crystallised calcium aluminate hydrates such as C_4AH_{13} and C_3AH_6 [13–16]. It seems that the crystal form of the hydrates principally depends on the MK/CH ratio and curing temperature. The presence of such hydration products shows that the pozzolanic reaction due to MK is thermoactivated as early as one day of age by thermal treatment [16].
- Studies on slag-based material in steam curing conditions are less widespread. In comparison with OPC cement (CEMI), OPC/slag binder with a lower *C/S* ratio produces more C-S-H and less portlandite, and increases the matrix compactness at long time [17]. Moreover, other hydrated phases are neoformed: alumino-ferrite monosulphate, secondary calcium silicate hydrates, a hydrotalcite-like phase, monocarbonate hydrogarnet [18–21]. But the initial hydration of slag is very slow (glass attack by hydroxide ions released during OPC hydration). Slag hydration is a chemical reaction with calcium hydroxide in presence of water which proceeds in the long term (progressive alkali release by slag at the same time as portlandite formation). With a thermal treatment, the solubility of portlandite decreases and the slag reactivity is greatly increased [22].

In the precast industry context, the cementitious material must have good mechanical properties at early age. Considering the environmental and economic problems that precast concrete makers are faced with when using CEM I cement, and in the light of the promising results obtained on steam cured mortars [12] and the hydration of low CO_2, economical binders, i.e. binary or ternary binders based on CEM I, the objective of this paper is to increase knowledge of the nature of the hydrated phases developed at one day of age in slag/cement binder and MK/cement binder subjected to steam curing conditions. An explanation is proposed for the previously observed variation of early compressive strength [12].

2. Experiments

2.1. Raw constituents

For the various binders studied, a CEM I cement (Ordinary Portland Cement, OPC) and two mineral admixtures (blast furnace slag, GGBS, and metakaolin, MK) were used. The chemical compositions of OPC, GGBS and MK are presented in Table 1.

Ordinary Portland Cement (OPC), CEM I 52.5R principally composed of clinker, was obtained from Lafarge, La Malle (France).

Blast Furnace Slag (GGBS) was a mineral admixture, a by-product of the steel industry (cast-iron manufacturing in blast furnace), and came from Fos/Mer (France).

Table 1
Physical properties and chemical compositions of OPC cement, GGBS and MK (suppliers' data).

Physical properties

	Specific gravity (g/cm^3)	Fineness (cm^2/g)	D_{50} (µm)
OPC	3.15	4300[a]	15.0
GGBS	2.90	4700[a]	/
MK	2.50	187,000[b]	11.5

Chemical compositions

	SiO_2	Al_2O_3	Fe_2O_3	CaO	MgO	K_2O	SO_3	LOI
OPC[c]	19.9	4.8	2.8	63.6	1.4	0.9	3.5	2.2
GGBS[c]	37.8	10.6	0.4	41.5	8.6	0.2	/	tr
MK[c]	56.2	37.2	1.4	1.2	0.2	1.2	/	2.1

[a] Blaine method.

[b] BET method.

[c] % weight, tr trace.

Metakaolin (MK) was MK commercially available in France (Pieri). This pozzolanic admixture is obtained from the slow calcination of kaolinite by the fluidised bed process [23]. It should be mentioned that the metakaolin used in this study was not pure. It was composed of 68% metakaolin, 13% quartz, 11% illite [16,24].

Binder combinations. Four combinations of the three raw constituents (OPC, GGBS, MK) were studied (B1 to B4). B1 binder was taken as the reference in this study: it presents high reactivity at early age, and guarantees good performance at 28 days according to European Standard EN 196-1 [4]. B1 and B3 binders are commercially available cements, named CEMI-52.5R and CEMII-A/S-52.5 N respectively in European standard designation [2]. They came from the same production site (La Malle) but differed in their clinker content: 18% of clinker by weight was replaced by GGBS (Fos/Mer) in CEMII-52.5 N. The replacement of 25% by mass of B1 or B3 with MK gave the B2 and B4 binders respectively.

The compositions of the four binders are given in Table 2.

2.2. Mixes

The cement paste mixes studied were composed of 500 g by mass of binder (Bi) and 175 g of water. They were named P1 to P4 in reference to the binders B1 to B4. The primary mix P1 contained only the B1 binder, P2 incorporated only B2 binder, etc. After mixing in the standardised sequence [4] in a mixer with 2-litre maximum capacity, each mixture was placed in cylindrical moulds (diameter = 30 mm, height = 50 mm) using vibration (48 Hz, 1.6 g).

2.3. Thermal treatment

Immediately after moulding, the paste cylinders were exposed to a simulated steam curing cycle with a maximum temperature of 55 °C and a total duration of 17.8 h. The cycle included 2.83 h of pre-setting at 30 °C, followed by 2.5 h of heating at 10 °C temperature increase per hour up to 55 °C, 12.5 h of exposure at 55 °C and a 2 h cooling down period. This thermal treatment corresponded to the average cycle used in precast factories.

After de-moulding (≈20 h), the paste samples were stored in water (20 °C ± 1 °C) up to the time of the tests.

2.4. Methods

2.4.1. Stopping of hydration

Freeze-drying was applied at 1 day of age. This is considered to be a rapid method for stopping hydration which also avoids sample carbonation. A crushed sample of a given paste Pi was first immersed in liquid nitrogen (−196 °C) for 5 min so that the water of the interstitial solution still available for hydration was changed into essentially amorphous ice. Next, the sample was placed in a freeze-dryer for 24 h in which temperature and vacuum pressure were kept to −40 °C and 13.3 Pa, respectively. This operation enabled the ice trapped in the paste porosity to be sublimated.

Table 2
Compositions of binder used in cementitious materials.

Designation	OPC[a]	GGBS[a]	MK[a]	
B1 (Binder 1)	100.0	0.0	0.0	CEMI-52.5R, commercially available (primary binder)
B2 (Binder 2)	75.0	0.0	25.0	75% CEMI-52.5R—25% MK, laboratory-made (binary binder)
B3 (Binder 3)	82.0	18.0	0.0	CEMII/A-S-52.5R; commercially available (binary binder)
B4 (Binder 4)	61.5	13.5	25.0	75% CEMII/A-S-52.5R—25% MK, laboratory-made (ternary binder)

[a] % weight.

2.4.2. Mineralogical analysis: XRD

The measuring instrument used for XRD worked with Co-Kα radiation ($\lambda_{K\alpha} = 1789$) at 40 kV and 30 mA. The 2-Theta values ranged from 4° to 70° and were recorded in 0.04° steps with a counting time of 10 s per step. The measurement was carried out on powder passing through a 40 µm sieve. The XRD technique identifies crystallised hydrated and anhydrous phases in a paste.

2.4.3. Thermal analysis: DTA and TGA

Differential thermal analysis (DTA) and thermogravimetric analysis (TGA) were used to qualitatively and quantitatively follow the hydration reactions [25,26].

For DTA, a crushed 40-µm powder specimen was placed in a refractory steel crucible and analysed at a heating rate of 5.8 °C/min up to 800 °C. Sample masses ranged from 1.00 to 1.10 g. In the case of TGA, the specimens (40-µm powder) were introduced into a quartz crucible and analysed at a heating rate of 7.5 °C/min up to 800 °C. The masses of the samples were between 200 and 220 mg.

DTA locates the temperature ranges corresponding to the thermal decomposition of different phases in a paste. The usual temperature intervals for the decomposition of the different phases in cement paste are as follows [27].

- [30–105 °C]: escape of the evaporable water and a part of the bound water, ettringite decomposition.
- [110–170 °C]: decomposition of gypsum (double endothermic reaction), ettringite, loss of part of water from the carbo-aluminate and aluminate hydrates and from C-S-H (100–180 °C).
- [180–350 °C]: loss of the rest of the bound water from the decomposition of hydrated calcium silica-aluminate.
- [500–570 °C]: dehydroxylation of portlandite.
- [700–900 °C]: decarbonation of calcium carbonate.

TGA measures the weight loss due to the various hydration product decompositions from ambient temperature to 800 °C. Three temperature intervals were investigated in this study. The first concerned the temperature range of 100–200 °C where C-S-H and hydrated gehlenite C_2ASH_8 decompose. This initial portion of the TG curves gave information about the amount of hydration products. The amount of hydrates of all binders could be assessed from the positions of their respective weight loss curves; the greater this weight loss, the greater the amount of hydration products in the paste. In the second temperature range [200 °C–500 °C], only the decomposition of aluminate hydrated phases (C_4AH_{13} and C_3ASH_6) were considered. The third temperature interval, from 500 °C to 570 °C in this study, was related to the decomposition of calcium hydroxide (CH). This phase could be quantified by the tangent method [28,29] and the progress of the pozzolanic reaction due to metakaolin could be evaluated.

In addition, the derivative dTG(%)/d*t* of each TG curve was calculated to quantify hydrated phases as C-S-H or calcium aluminate hydrate (C-A-H) or calcium silico-aluminate hydrate (C-A-S-H) [30]. Spectra obtained from dTG(%)/d*t* = f(T°C) curves were deconvolved to determine the area of each hydrate decomposition according to the method of Lorentzian area deconvolution from the amplitude a_0, the centre a_1 and the width (>0) a_2 (Eq. (2)) [31]. Fig. 1 illustrates the method of quantification for C-S-H.

$$\frac{dTG(\%)}{dt} = \frac{a_0}{1 + \left(\frac{T - a_1}{a_2}\right)^2} \tag{2}$$

With:

dTG(%)/d*t*	derived value of TG(%) with respect to time *t*,
T	temperature,
a_0, a_1 and a_2	amplitude, centre and width (>0) of the peak, respectively.

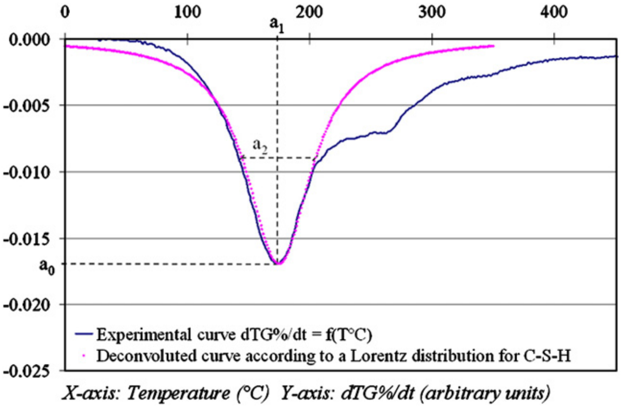

Fig. 1. Deconvolution method for an approximate quantification of C-S-H, C-A(S)-H and CH obtained from dTG%/d*t* curves.

It is important to note that thermograms were plotted up to 650 °C for DTA, TGA and dTG%/d*t* curves in Section 3 because, beyond these temperatures, there was no information that was useful for the present study. The freeze-drying treatment of samples prevented their carbonation, and so no trace of calcium carbonate was detected during analysis.

2.4.4. Chemical analysis: electronic microprobe

Crushed pieces of paste were moulded in epoxy resin. After polymerisation of the resin, the samples were polished with a lubricant containing no water, metallized and analysed.

To chemically characterise the various pastes, analyses (40 points for each sample) were carried out on a 10 µm^3 representative volume of hydrated phase [32]. The results were given as the molar percentage of oxide: CaO, SiO_2, Al_2O_3, Fe_2O_3 (major oxides), SO_3, Na_2O, K_2O, MgO, MnO (minor oxides) and TiO_2 (checking). Only CaO, SiO_2 and Al_2O_3 were used in this study. In particular, we studied:

- the variation of average values of CaO/SiO_2 molar ratio (*C*/*S*);
- the variation of chemical composition in the CaO–SiO_2–Al_2O_3 system; the results presented on ternary diagrams were normalised because the sum of the proportions of the three major oxides was always less than unity (variation from 62% to 92% in hydration products);
- the variation of Al content versus Na or K content.

3. Analysis of the hydrated phase at one day of age according to the nature of the binder in steam curing conditions: results and discussion

3.1. Mineralogical analysis: identification of crystallised phases

Fig. 2 shows the X-ray diffraction patterns for the reference paste (P1) and the pastes made with binary binders (P2 and P3) and ternary binder (P4). Several observations and comments can be made.

- The evolution of calcium hydroxide consumption (noted P on Fig. 2) relative to the pozzolanic reaction can be assessed by considering the main diffraction peak at about 2θ = 39.7° (2.63 Å) and the secondary diffraction peak at about 2θ = 20.9° (4.91 Å) [25]. Fig. 2 shows that, as early as 1 day of age, CH consumption was evident in pastes containing MK (P2 and P4. This observation suggests that the pozzolanic reaction through CH consumption has occurred at one day of age when MK is incorporated.
- The diffraction peak at about 2θ = 12.1° corresponds to the C_4AH_{13} hydrate (noted V) which is isostructural with portlandite and belongs to the AFm family. The peak is weakly perceptible in all cases.

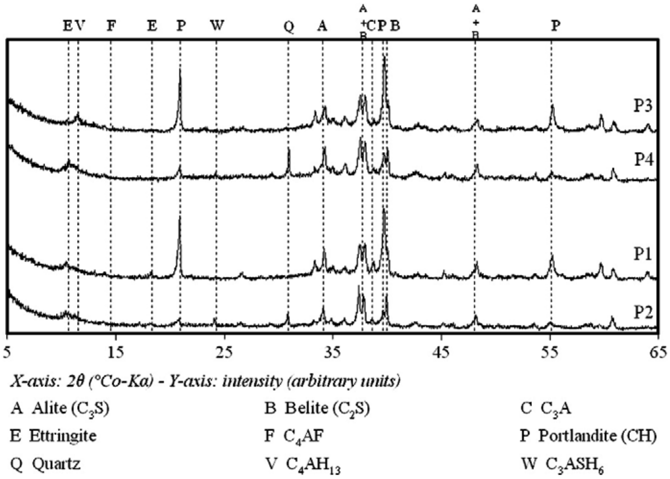

A Alite (C_3S)	B Belite (C_2S)	C C_3A
E Ettringite	F C_4AF	P Portlandite (CH)
Q Quartz	V C_4AH_{13}	W C_3ASH_6

Fig. 2. XRD diagrams of P1, P2, P3 and P4 pastes at 1 day of age.

- Hydrogarnet C_3ASH_6 (W on Fig. 2) is present in paste incorporating MK (P2 and P4) as indicated by a diffraction peak at about 2θ = 23.9° [14,15].
- Except for P3 (clinker + GGBS-based paste), ettringite (E) is visible according to the diffraction peak at about 2θ = 10.6°.
- Quartz (Q), detected at about 2θ = 30.9° (3.36 Å) in P2 and P4 pastes, comes from impurities present in the MK.

These observations show that some differences in the nature of the hydration products were detected by means of XRD when MK was incorporated in steam cured cementitious materials. Compared to plain paste (P1) or GGBS-based paste (P3), the development of C_3ASH_6 phases was observed and, at the same time, the amount of calcium hydroxide was reduced in spite of the decrease in lime solubility with increasing temperature [33].

3.2. Thermal analysis: qualification and quantification of hydrated phases

3.2.1. Differential thermal analysis (DTA): identification of amorphous phases

Fig. 3 shows the DTA curves for steam cured pastes P1 (primary CEMI binder), P2 and P3 (binary binders) and P4 (ternary binder). The DTA curves present a similar form between P1 and P3 and between P2 and P4, suggesting two groups can be distinguished depending on whether metakaolin is incorporated (P2, P4) or not (P1, P3). The curves for P1 and P3 pastes show three marked endothermic reactions; the first two concern the temperature range of 100–180 °C (T_1 to T_2) corresponding to the decomposition of hydrated

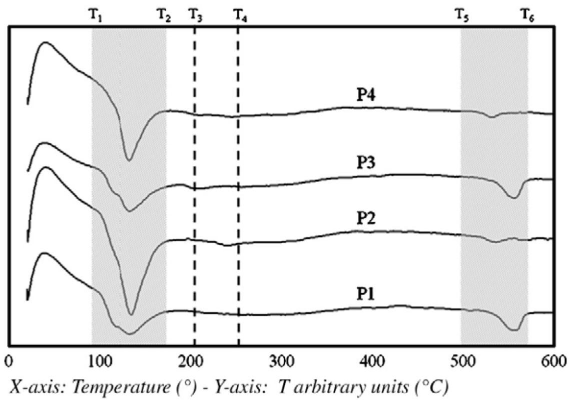

Fig. 3. DTA diagrams for P1, P2, P3 and P4 pastes at 1 day of age.

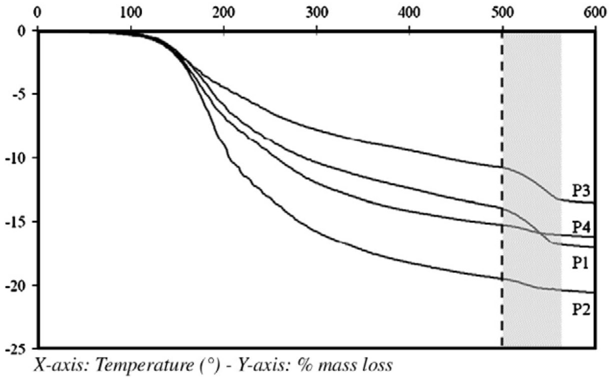

Fig. 4. TGA diagrams for P1, P2, P3 and P4 pastes at 1 day of age.

aluminates and C-S-H; the third one ranges from 500 °C to 570 °C (T_5 to T_6) and is associated with portlandite decomposition.

For P2 and P4 (MK-based pastes), the DT curves clearly show two endothermic reactions even though the CH peak is not very marked. The decomposition of C-S-H and hydrated gehlenite probably (T_3–T_4 temperature interval) can be observed. For these peaks, the intensity is greater in P2 and P4 than in P1 and P3. The variation of temperature (*X*-axis) and intensity (*Y*-axis) of the peaks for P2 and P4 in comparison with P1 and P3 show a difference concerning the structural homogeneity of C-S-H. When considering the temperature interval from 500 to 570 °C (i.e., T_5 to T_6), the decomposition of CH is less observable in P2 and P4 pastes than in P1 and P3 pastes, certainly due to CH consumption by the pozzolanic reaction induced by MK.

Furthermore, it can be observed that the endothermic peaks with the lowest intensity are associated with hydrated gehlenite for P3 and P4 ($T_3 = 205$ °C) [34,35], and hydrated calcium aluminate (C_4AH_{13}) for P2 and P3 ($T_4 = 245$ °C).

3.2.2. Thermogravimetric analysis (TGA): quantification of CH

The TGA curves plotted in Fig. 4 quantify the weight loss due to decomposition of hydrated phases for the four steam cured pastes at 1 day of age. Two temperature intervals were investigated regarding the evolution of hydrated phases in this study (pozzolanic reaction and slag hydration) [25].

The first interval [100–500 °C] corresponds to the decomposition of the calcium silicate hydrate phase (C-S-H) and calcium silicate aluminate hydrates (C-A-S-H), probably hydrated gehlenite (C_2ASH_8). Table 3 presents the total percentage of mass loss per kg of material up to 500 °C, calculated from the TG curves (Fig. 4).

The second interval [500–570 °C], related to the decomposition of portlandite (CH), could be quantified and the progress of the pozzolanic reaction evaluated. The molar amount of portlandite per kg of material at 1 day of age, deduced from thermogravimetric curves by the use of the tangent method [28,29], is shown in Table 4.

Based on the above preliminary remarks, some observations and comments can be made.

- For a temperature of decomposition up to 500 °C (Table 3), the amount of hydrated phases was significantly greater in MK-based pastes (P2 and P4) than in the other pastes (P1 and P3). The smallest amount was observed when only slag was incorporated (P3). Taking into account the dilution effect due to clinker replacement with a mineral admixture, and in comparison with paste P1 (clinker alone), the use of the clinker + MK combination (P2 paste) or ternary binder clinker + slag + MK (P4 paste) significantly increased the amount of hydrates, by 86% and 78%, respectively.
- When MK was incorporated in replacement of OPC cement (P2) or the OPC/slag combination (P4), there was a decrease in the amount of portlandite (500 °C–570 °C interval) in all cases. It can be observed that the consumption of CH was due to the pozzolanic reaction occurring when MK was incorporated rather than the hydration of slag (1.14 molar quantity consumed by the pozzolanic reaction to be compared with the 0.02 value related to slag hydration in Table 4).

The above observations are consistent with XRD and DTA results indicating that the pozzolanic reaction, thermoactivated in steam curing conditions, occurs as early as 1 day of age. Accordingly, the increase in C-S-H and C-S-A-H quantities was as expected for P2 and P4 pastes.

Table 3

Average percentage mass loss per kg of material in steam cured pastes at 1 day of age with standard deviation (measurements from 3 samples up to a decomposition temperature of 500 °C on TG curves).

	% mass loss measured	% mass loss calculated for equivalent OPC content (reference = P2, 75.0%)	% mass loss calculated for equivalent OPC content (reference = P3, 82.0%)	% mass loss calculated for equivalent OPC content (reference = P4, 61.5%)
P1	13.96 (±0.55)	13.96	13.96	13.96
P2	19.50 (±0.89)	26.00	/	/
P3	10.94 (±0.22)	/	13.34	/
P4	15.31 (±0.36)	/	/	24.89
% mass loss due to :				
Pozzolanic reaction (P2–P1 in column 3)				12.04
Slag reaction (P3–P1 in column 4)				−0.62
Both pozzolanic and slag reactions (P4–P1 in column 5)				10.93

Table 4

Average molar quantity of portlandite per kg of material in steam cured pastes at 1 day of age, with standard deviation (measurements from 3 samples).

	nCa(OH)$_2$ measured	nCa(OH)$_2$ calculated for equivalent OPC content (reference = P2, 75.0%)	nCa(OH)$_2$ calculated for equivalent OPC content (reference = P3, 82.0%)	nCa(OH)$_2$ calculated for equivalent OPC content (reference = P4, 61.5%)
P1	1.57 (±0.014)	1.57	1.57	1.57
P2	0.32 (±0.015)	0.43	/	/
P3	1.27 (±0.011)	/	1.55	/
P4	0.13 (±0.009)	/	/	0.21
nCa(OH)$_2$ consumed by:				
Pozzolanic reaction (P1–P2 in column 3)				1.14
Slag reaction (P1–P3 in column 4)				0.02
Both pozzolanic and slag reactions (P1–P4 in column 5)				1.36

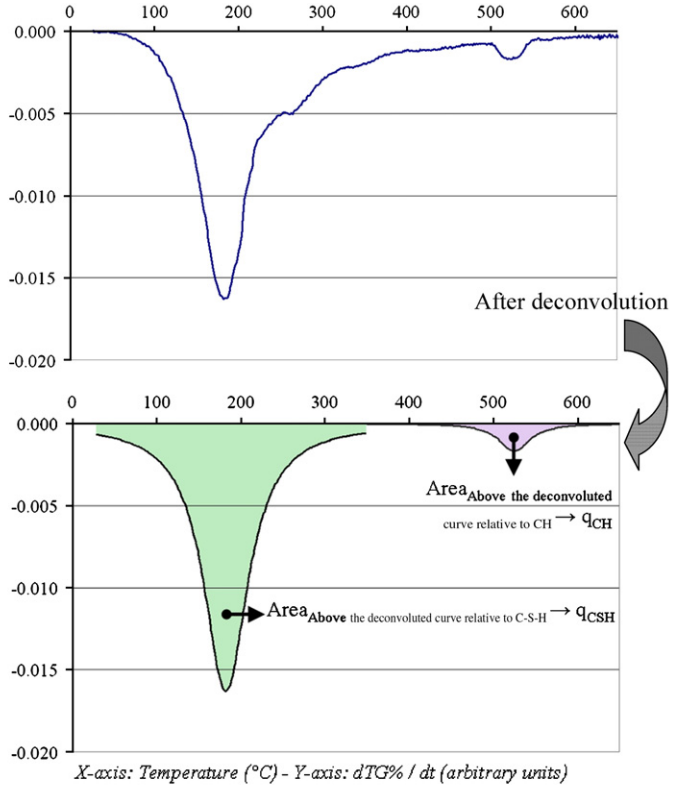

Fig. 5. Calculation of amount of hydrates by deconvolution method with dTG%/d*t* curves.

3.2.3. Time derivative of TG curves (dTG/dt): quantification of C-S-H and CH

To quantify the amounts of the hydrated phases, the time derivatives of TG curves (dTG/d*t*) were used [30]. The derivatives were obtained from the gravimetric thermograms shown in Fig. 4.

The amount of hydrates can be obtained manually (Eq. (2)) from the deconvolved dTG/d*t* curve. The quantity for each hydrate (q_{CSH}, q_{CH}) corresponds to the area under the deconvolution curve. Fig. 5 illustrates the method for calculating the hydrated phase.

The C-A-S-H and C-A-H phases, difficult to dissociate, were not taken into account. Fig. 6 presents dTG/d*t* diagrams within the 0–650 °C temperature range for the four pastes P1 to P4 and their deconvolutions. Table 5 gathers together the amount of hydrates (C-S-H and CH) contained in steam cured pastes at 1 day of age and the associated temperatures of hydrate decomposition defined at the centre of each peak coming from the deconvolution.

3.2.3.1. Temperature of decomposition. The temperature of decomposition of each hydrate can be associated with the centre of a discriminated peak after deconvolution on the *X*-axis (a_1 value in Fig. 1). For a given hydration product, the temperature of decomposition (T_d) differs from one paste to another. It is interesting to note that the binder B3 (CEMI + GGBS) generates C-S-H phase with the smallest T_d, probably explained either by smaller hydrate particles or a weaker and less stable structure. When MK is incorporated (P2 and P4 pastes), CH phase has the smallest T_d.

3.2.3.2. Variation of the amounts of hydrates. In the following, only the amounts of C-S-H, and CH are considered. More information can be obtained when hydrated phases are discriminated because their intrinsic strengths are markedly different. It is well known that calcium silicate hydrate (C-S-H) is a mechanically strong phase, more resistant than hydrated calcium aluminate or silico-aluminates (C-A-H or C-A-S-H) [36] and portlandite (CH) which has a low strength because of its lamellar structure.

From Table 5, it can be seen that the amount of C-S-H gel is the greatest when MK-based binder is used, with or without GGBS (P4 and P2 respectively). The smallest amount of C-S-H is observed for GGBS/OPC based paste (P3), which confirms that the B3 binder

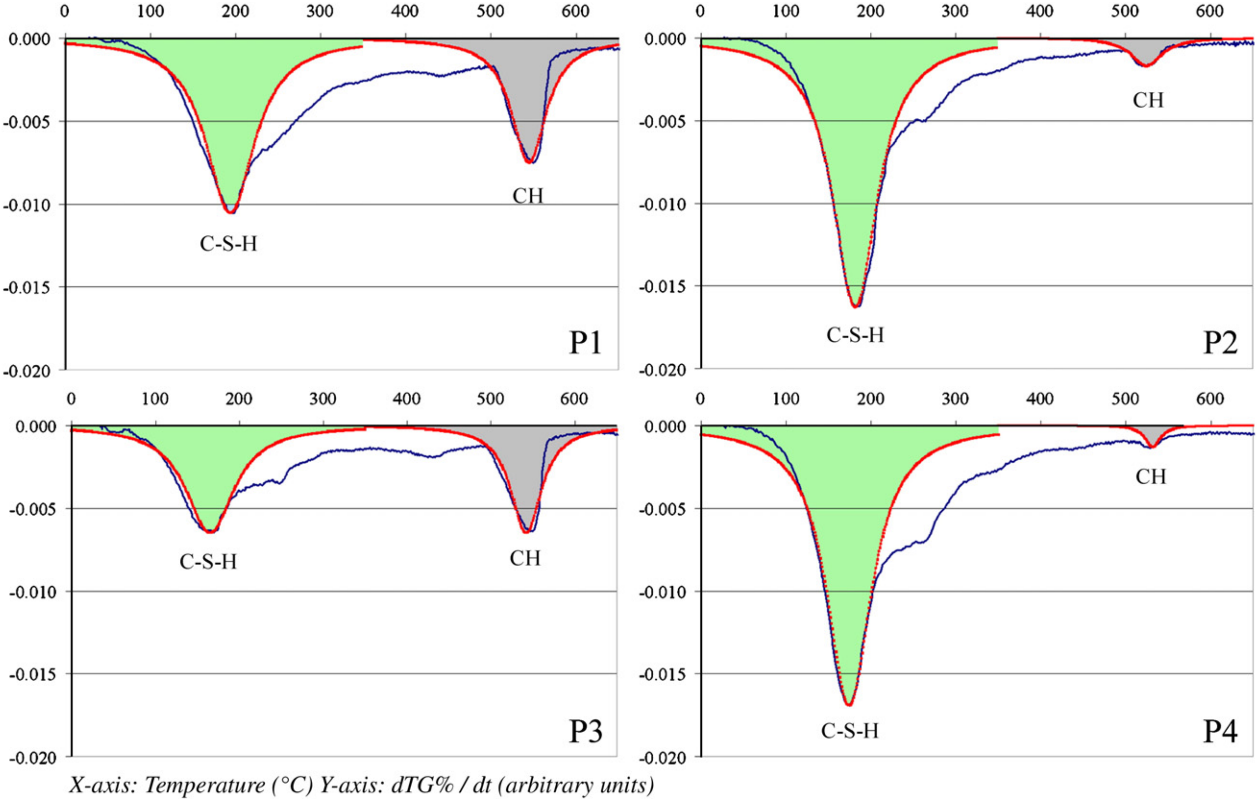

Fig. 6. dTG%/d*t* curves for P1, P2, P3 and P4 pastes at one day of age, and discriminated peaks after deconvolution.

Table 5
Quantity of hydrates (arbitrary units) contained in steam cured pastes at 1 day of age and associated temperatures of hydrate decomposition Td (in brackets).

	Hydrates identified with C-S-H (noted q_{CSH})	Hydrates identified with CH (noted q_{CH})
P1	1.01 ± 0.029 (194 ± 3.8 °C)	0.52 ± 0.022 (548 ± 3.6 °C)
P2	1.45 ± 0.024 (183 ± 5.1 °C)	0.11 ± 0.006 (524 ± 5.1 °C)
P3	0.68 ± 0.035 (163 ± 2.1 °C)	0.41 ± 0.020 (543 ± 2.1 °C)
P4	1.51 ± 0.0.38 (175 ± 3.0 °C)	0.04 ± 0.006 (532 ± 3.0 °C)

(CEMII = CEMI + GGBS) is less reactive than B1 binder (CEMI only) at early ages, as shown by the compressive strength results obtained previously [12] (see Appendix 1).

In the case of portlandite (CH) formation, the results of deconvolved (dTG/d*t*) curves confirm those obtained from thermogravimetric analysis (Section 3.2.2): MK-based pastes (P2 and P4) show the smallest amount of CH.

At this step, thermal analyses demonstrate an increase in the amount of C-S-H phase existing in MK-based pastes with or without GGBS. Hence, the difference in the amount of the hydrated phase cannot completely explain the variation of strength at 1 day of age when MK is incorporated. These observations are in agreement with Love's results [37].

3.3. Chemical analysis: evolution of chemical composition

3.3.1. Variation of molar C/S ratio

Table 6 presents the average values of the experimental molar CaO/SiO_2 ratio (*C*/*S*) measured in hydrated areas at 1 day of age by means of a microprobe and the theoretical CaO/SiO_2 ratio calculated from chemical compositions of anhydrous binders (mass average).

The following observations and comments can be made.

- The *C*/*S* ratio is always greater than 2.5 in pastes without MK (P1 and P3); it is not significantly different between P1 and P3.
- When MK is incorporated, the *C*/*S* ratio is decreased and is less than 2.0.
- The similarity between experimental and theoretical C/S ratios (Table 6) suggests a homogeneous distribution of the hydration products as micro-crystals around remaining cement and metakaolin particles. This is consistent with one of the two hypotheses explaining lower decomposition temperature values when MK and GGBS are incorporated (Section 3.2.3).

3.3.2. Variation of proportions of CaO, SiO_2, Al_2O_3

The ternary composition by major oxides (CaO, SiO_2, Al_2O_3) in anhydrous phases, and hydrated phases developed in each paste Pi, is shown in Figs. 7–11. As regards P1 and P3, some comments can be made.

- A very narrow scatter plot representing hydrates is visible in P1 paste (set I in Fig. 8). These hydration products can be assimilated to the high and variable *C*/*S* ratio calcium silicate hydrates, a blend of C-S-H and portlandite and only portlandite. The Al_2O_3 content is low in accordance with the composition of B1 binder (Fig. 7).
- The same tendency also exists in P3 paste (set III in Fig. 10) although a greater dispersion is observed. Few points associated with portlandite phase are visible, indicating that portlandite may be consumed by slag hydration, thermoactivated at early age.

Table 6
Variation of *C*/*S* ratios of binders.

	P1	P2	P3	P4
Measured with microprobe analysis (calculated from hydrated phases)	3.31 ± 0.89	1.57 ± 0.77	2.99 ± 0.71	1.40 ± 0.88
Theoretical (calculated from chemical compositions of anhydrous binders)	3.20	1.66	2.58	1.43

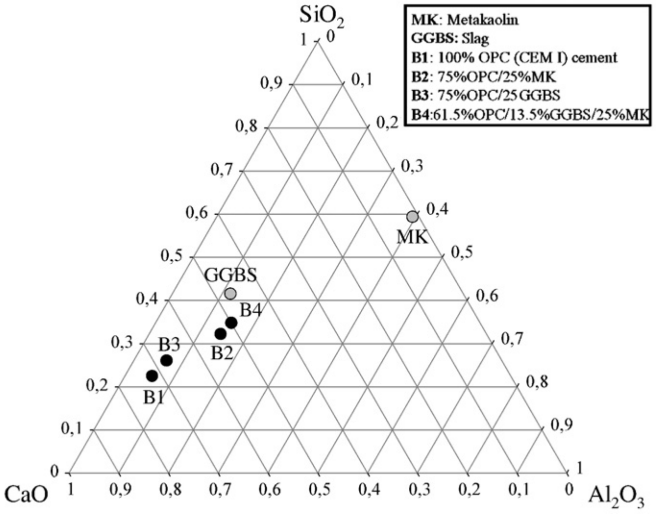

Fig. 7. Molar proportions of the major CaO, SiO_2, Al_2O_3 elements—raw materials and binders.

When MK is incorporated in steam cured pastes (P2 and P4), the following points can be noted.

- A variation of the hydrated phase composition is clearly evidenced: more silica (SiO_2) and alumina (Al_2O_3) are included and a decrease in the calcium oxide content is observed (Figs. 9 and 11). Accordingly, the ellipsoid of the scatter plot has a more elongated shape toward SiO_2 and Al_2O_3 showing new families of hydrated phases, probably secondary C-S-H [37] and C-S-A-H, i.e. C-S-H with a higher Al_2O_3 content than C-S-H coming from clinker hydration [38,39,40]. The points assimilated with the portlandite on Figs. 8 and 10 are no longer visible; CH is consumed by pozzolanic reaction due to the presence of MK in P2 paste (Fig. 9) and by the coupling of slag hydration and pozzolanic reaction in P4 paste (Fig. 11).
- The incorporation of GGBS (Fig. 11) leads to an evolution, with an increase in the CaO content.

3.3.3. Substitution of {$Al^{3\pm} \pm Na^{\pm}/K^{\pm}$} for $Si^{4\pm}$

In the literature [38,39,40], a possible substitution of aluminium Al^{3+} is shown for silicon Si^{4+} in C-S-A-H phases. Within such

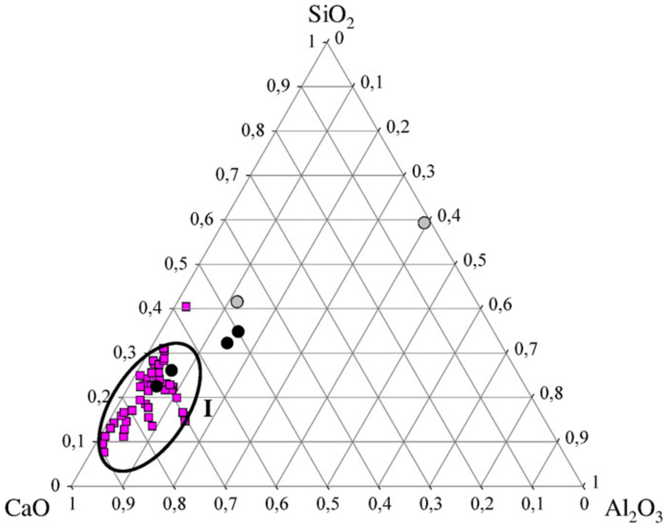

Fig. 8. Molar proportions of the CaO, SiO_2, Al_2O_3 major elements—P1 paste.

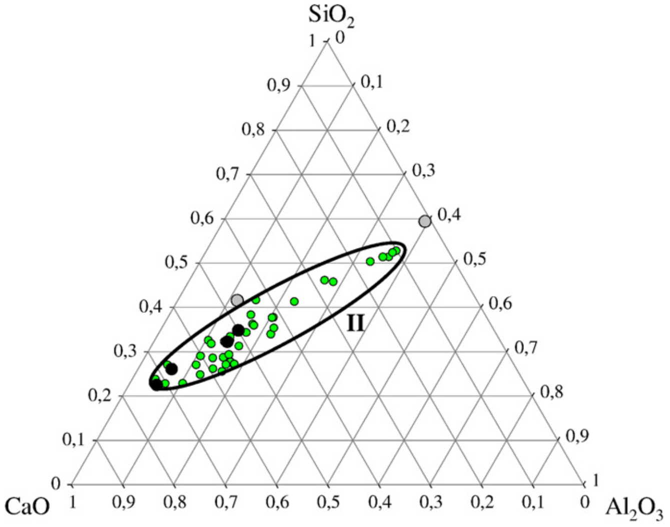

Fig. 9. Molar proportions of the CaO, SiO_2, Al_2O_3 major elements—P2 paste.

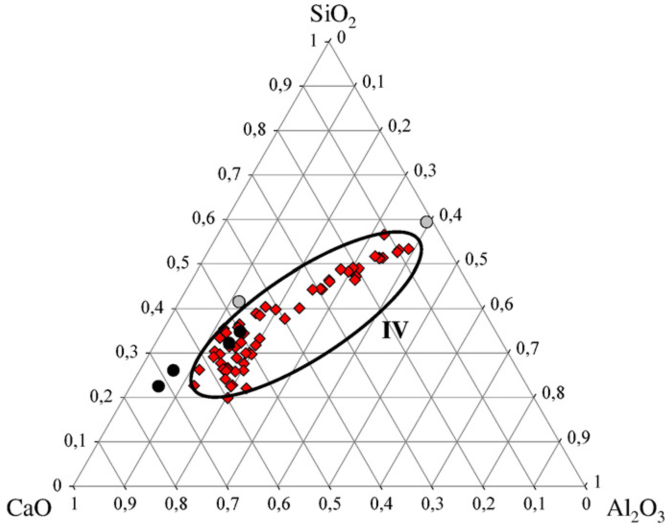

Fig. 11. Molar proportions of the major CaO, SiO_2, Al_2O_3 elements—P4 paste.

hydration products, the conservation of valence electronic structure existing in C-S–H is possible via the insertion of monovalent cations. This fact is confirmed when Al content is plotted versus Na or K content: strong positive correlations are observed when MK is incorporated (P2 and P4 in Fig. 12) while they are not present in other cases (P1 and P3 in Fig. 12).

4. Conclusion

Binders that are very reactive at early ages are necessary in the precast industry to achieve sufficient strength at the time when concrete elements are prestressed and ensure daily profitability. To that end, CEMI 52.5R cement (OPC), known to be reactive at early age, is currently used in combination with steam curing. But the use of CEMI containing a large amount of clinker (at least 95% by weight) is a real problem because of the high CO_2 emissions resulting from clinker production (1 ton of clinker produced ≈1 ton of CO_2 released into the atmosphere). An alternative to the progressive decrease in the production of CEM I to protect the environment would be the partial replacement of CEM I by mineral admixtures such as metakaolin (MK) and/or blast furnace slag (GGBS).

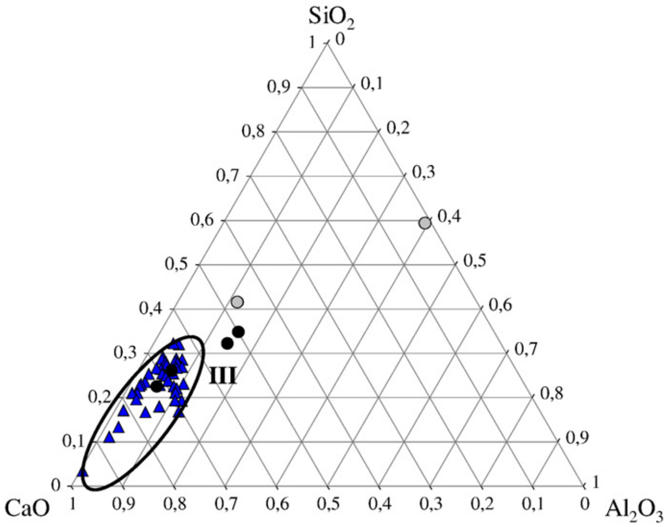

Fig. 10. Molar proportions of the major CaO, SiO_2, Al_2O_3 elements—P3 paste.

The present study tried to connect, at one day of age, the compressive strength of steam cured mortars made with various binders [12] and the hydration of these binders. The progress of hydration was characterised by means of XRD, thermal and microprobe analyses. Four binders were studied:

- Primary binder B1 (100%CEMI 52.5R) defined as the reference binder;
- Secondary binders B2 (75%CEMI + 25%MK) and B3 (82%CEMI + 18%GGBS);
- Ternary binder B4 (61.5%CEMI + 13.5%GGBS + 25%MK).

In comparison with the compressive strength of reference mortar (33.9 MPa) incorporating only B1 binder, and in comparison with the corresponding hydration of B1, the following conclusions can be drawn.

- The 25% replacement by mass of CEM I cement with MK (B2 binder) generated a relative increase in strength of 39%. An explanation lies in the thermoactivation of the pozzolanic reaction due to MK as early as one day of age. The occurrence of such a reaction is associated with a significant consumption of portlandite (−73%) and an increase in the amount of calcium silicate hydrate phase (+44% for C-S-H). The substitution of Si^{4+} for the Al^{3+} from aluminium oxide present in MK explains the formation of C-A-S-H phases. A decrease in the molar *C*/*S* ratio (−53%), an enrichment of SiO_2 and Al_2O_3 oxides are also observed in hydration products developed in MK-based material. In addition, an increase in the temperature of decomposition indicates that these products are more stable than those generated from B1 binder.
- The 18% replacement by mass of CEM I cement with GGBS (B3 binder) involved a 19% decrease in strength. This observation is consistent with the significant decrease in the amount of hydrated phase, in particular C-S-H (−33%). Despite the steam curing condition, the slag hydration is not much developed (−1% for CH consumption). Few changes are observed in the chemical nature distribution of hydration products: only weak decreases in *C*/*S* ratio (−10%).
- The ternary binder B4 enabled a 31%-increase in strength. In that case, the hydration showed similarities with that in CEMI/MK binder (B2), indicating that the main differences in the hydration

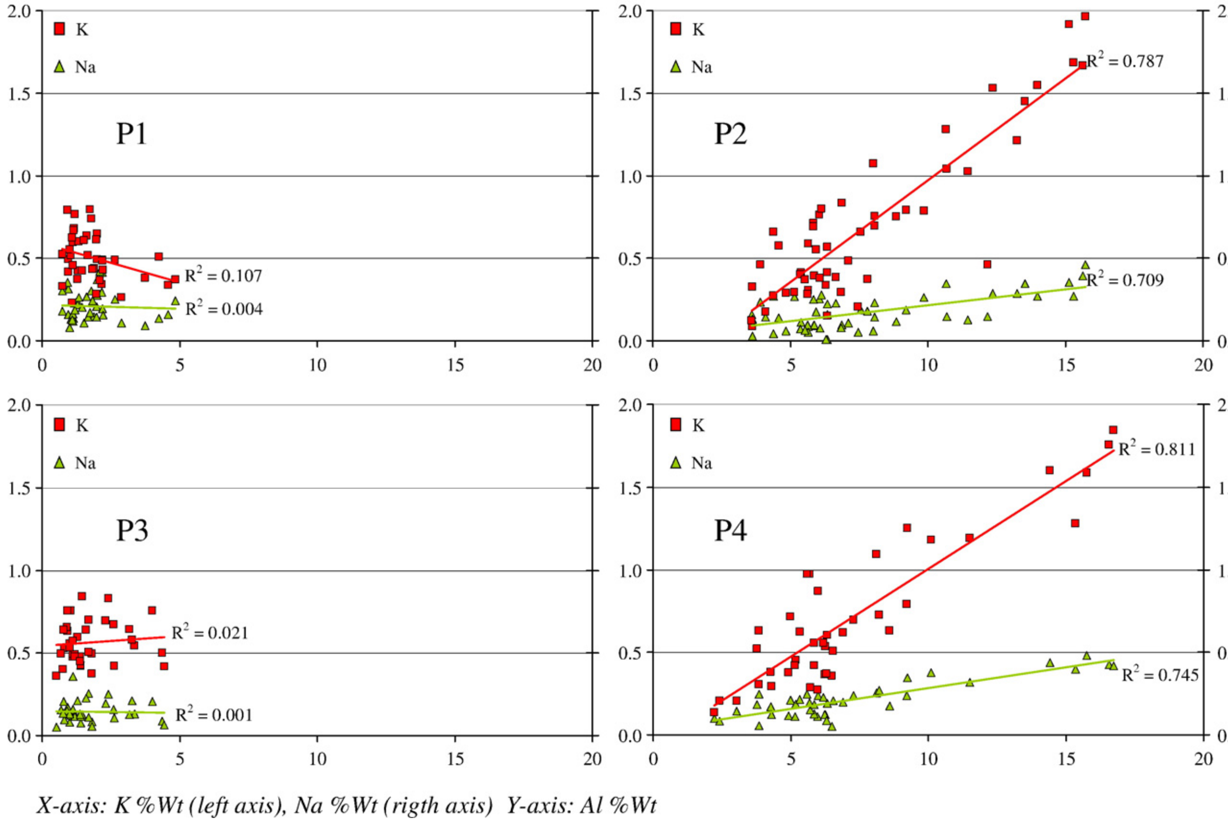

Fig. 12. Variation of Al content versus Na or K content (%wt.).

of CEM I or CEMI/GGBS binders are due to the metakaolin in steam curing conditions. A decrease in the amount of portlandite due to pozzolanic reaction (−87%), an increase in C-S-H amounts (+49%), a decrease in *C/S* ratio (−58%) are noted.

Finally, the various results collected in this work suggest that the use of clinker/MK or clinker/GGBS/MK combinations as a binary or ternary binder, respectively, is of interest in the context of the precast industry. The partial replacement of such systems with MK improves the quality and the amount of the hydrated phase. Accordingly, an increase in strength is observed. Environmentally speaking, the use of a clinker/GGBS/MK combination is positive; there is a saving of clinker, which implies a reduction in the CO_2 released into the atmosphere. Hence, the prospects for phasing out CEMI 52.5R or Ordinary Portland Cement (OPC) and using low-CO_2 binder such as a cement/MK combination are realistic.

Acknowledgements

The authors are very grateful to the enterprise SEAC-Gf and the Association Nationale de la Recherche Technique (ANRT) for supporting the present research. They also wish to thank Professor JP. Fortuné and P. Broilliard for helpful discussions.

Appendix 1. Compressive strength measured on steam cured mortars at 1 day [12]

Mortar	Design of binder *Bi*	Compressive strength (MPa) and standard deviation
M1	B1 = 100% CEMI 52.5R	33.9 (±0.96)
M2	B2 = 75% CEMI + 25%MK	47.1 (±0.56)
M3	B3 = 82% CEMI + 18%GGBS	27.5 (±0.75)
M4	B4 = 61.5% CEMI + 13.5%GGBS + 25%MK	44.3 (±0.73)

Appendix 2. Hydration products of steam cured binder incorporating MK or slag at 1 day

MK-based cement pastes		
References	Binder	Hydrates
[13]	MK-lime matrix, w/s = 0.8, 55 °C (1:6)	C-S-H, HG, CH.
	(1:3)	C-S-H, C_4AH_{13}, HG, CH.
	(1:1.5)	C-S-H, GH, HG, CH(tr).
	(1:1,75)	C-S-H, GH, C_4AH_{13}.
	(1:0.40)	C-S-H, GH.
[14]	MK-lime matrix, (1:1), w/s = 2.37, 60 °C	C-S-H, C_4AH_{13}, GH, CH.
[15]	MK/OPC paste w/s = 0.55, 60 °C 10%MK	C-S-H, GH, C_3ASH_6(tr), CH, $Ca_4Al_2O_6(CO_3)0.5(OH)11.5H_2O$(tr)
	20%MK	C-S-H, GH, CH.
	25%MK	C-S-H, GH, CH.
[16]	MK/OPC paste (1:3), w/s = 0.35, 55 °C	C-S-H, C_4AH_{13}, HG, GH, CH.
Slag-based cement pastes		
References	Binder	Hydrates
[18]	Slag-OPC paste (2:3) w/s = 0.5, 30 °C	C-S-H, Afm, HP, CH, Et
[19]	Slag-OPC paste (2:3) w/s = 0.5, 60 °C	C-S-H, Afm, HP, CH
[20,21]	Slag-OPC paste (1:3) w/s = 0.48, 95 °C	CSH, CSH_{II}, HP, MC, HG.

Afm: monosulphoaluminate, CH: portlandite, C-S-H: calcium silicate hydrate, C-S-H_{II}: secondary calcium silicate hydrate, Et: ettringite, GH: hydrated gehlenite (C_2ASH_8), HG: hydrogarnet (C_3ASH_6), HP: hydrotalcite-like phase, MC: monocarbonate.
w/s: water/solid ratio, (1:1): ratio of constituent proportions by mass, tr: trace.

References

[1] FIB (International Federation of Concrete), http://www.fib.org, Internet site of International Federation of Concrete, 2007.

[2] EN 197-1 (European Norm), Cement—Part 1: Composition, specifications and conformity criteria for common cements, AFNOR Association Française de Normalisation (Eds), 2001.

[3] FM. Lea, PC. Hewlett, Lea's Chemistry of Cement and Concrete, 4th Edition, Published by Elsevier, Butterworth-Heinemann (Eds), 1998.

[4] EN 196-1 (European Norm), Method of testing cement—Part 1: Determination of strength, AFNOR Association Française de Normalisation (Eds), 2006.

[5] S. Pihlajavaara, Effect of temperature on strength of concrete, American Concrete Institute Special Publication; 34 (1972) 347–434.

[6] P. Klieger, Effect of mixing and curing temperature on concrete strength, Journal American Concrete Institute 54 (6) (1954) 1063–1081.

[7] G.J. Verbeck, R.H. Helmuth, Structures and physical properties of cement pastes, Proceedings of the 5th International Symposium on the Chemistry of Cement, Tokyo Japan, 1968, pp. 1–32.

[8] AFNOR (Association Française de Normalisation), Ciment et chaux: Recueil de normes, AFNOR (Eds), Paris, 2003.

[9] AM. Neville, Properties of concrete, Eyrolles (Eds), 2000.

[10] E. Gartner, Industrially interesting approaches to "low-CO2" cement, Cement and Concrete Research 34 (2004) 1489–1498.

[11] Kyoto Protocol, The United Nations framework convention on climate change, Kyoto Japan, 1990.

[12] F. Cassagnabère, M. Mouret, G. Escadeillas, P. Broilliard, Low CO2 binder: a solution for precast industry, Concrete structure Simulators of development, Fib symposium, Dubrovnik, Croatia, 2007.

[13] P.S. Silva, F.P. Glasser, Phase relation in the system CaO–Al2O3–SiO2–H2O relevant to MK–Calcium hydroxide hydration, Cement and Concrete Research 23 (3) (1993) 627–639.

[14] M. Frias Rojas, J. Cabrera, The effect of temperature on the hydration rate and stability of the hydration phases of MK–lime–water systems, Cement and Concrete Research 32 (1) (2002) 133–138.

[15] M. Rojas, M.I. Sanchez de Rojas, The effect of high curing temperature on the reaction kinetics in MK/lime and MK-blended cement matrices at 60°C, Cement and Concrete Research 33 5 (2003) 643–649.

[16] F. Cassagnabère, G. Escadeillas, M. Mouret, Study of the reactivity of cement/metakaolin binders at early age for specific use in steam cured precast concrete, Construction and Building Materials 23 (2009) 775–784.

[17] J. Duchesne, M.A. Bérubét, Effect of supplementary cementing materials on the composition of cement hydration products, Advanced Cement Based Materials 2 (1995) 42–53.

[18] J.I. Escalante, L.Y. Gomez, K.K. Johal, G. Mendoza, H. Mancha, J. Mendez, Reactivity of blast-furnace slag in Portland cement blends hydrated under different conditions, Cement and Concrete Research 31 (2001) 1403–1409.

[19] J.I. Escalante-Garcia, J.H. Sharp, The microstructure and mechanical properties of blended cements hydrated at various temperatures, Cement and Concrete Research 31 (2001) 695–702.

[20] T. Ramlochan, P. Zacarias, M.D.A. Thomas, R.D. Hooton, The effect of pozzolans and slag on the expansion of mortars cured at elevated temperature: Part I: Expansive behaviour, Cement and Concrete Research 33 (2003) 807–814.

[21] T. Ramlochan, P. Zacarias, M.D.A. Thomas, R.D. Hooton, The effect of pozzolans and slag on the expansion of mortars cured at elevated temperature: Part II: Microstructural and microchemical investigations, Cement and Concrete Research 34 (2004) 1341–1356.

[22] B. Sioulas, J.G. Sanjayan, Hydration temperature in large high-strength concrete columns incorporating slag, Cement and Concrete Research 30 (2000) 1791–1799.

[23] S. Salvador, Production de pouzzolanes de synthèse par calcinations flash de sols argileux: etude des produits et conception d'une installation, PhD thesis, INSA Toulouse, France, 1992.

[24] F. Cassagnabère, Produits préfabriqués en béton filé: Vers l'amélioration des performances du matériau pour mieux gérer le procédé de production, PhD thesis, Toulouse University, France, 2007.

[25] S. Wild, J.M. Khatib, Portlandite consumption in metakaolin cement pastes and mortars, Cement and Concrete Research 27 (1996) 137–146.

[26] N. Saikia, S. Kato, T. Kojima, Thermogravimetric investigation on the chloride binding behaviour of MK–lime paste, Thermochimica Acta 444 (2006) 16–25.

[27] B.B. Sabir, S. Wild, J. Bai, Metakaolin and calcined clays as pozzolans for concrete: a review, Cement Concrete Composites 23-6 (2001) 441–454.

[28] B.K. Marsh, R.L. Day, Pozzolanic and cementitious reactions of fly ash in blended cement pastes, Cement and Concrete Research 18-2 (1988) 301–310.

[29] H.F.W. Taylor, Cement chemistry. 2nd ed, 1997.

[30] D.S. Klimesch, A. Ray, Use of the second-derivative differential thermal curve in the evaluation of cement-quartz with metakaolin addition autoclaved at 180 C, Thermochimica Acta 307 (1997) 167–176.

[31] N. Chapleau, C. Mangavel, J.P. Compoint, M. de Lamballerie Anton, Effect of high-pressure processing on myofibrillar protein structure, Journal of the Science of Food and Agriculture 84 (2003) 66–74.

[32] A. Bertron, G. Escadeillas, J. Duchesne, Cement pastes alteration by liquid manure organic acids: chemical and mineralogical characterization, Cement and Concrete Research 34 (2004) 1823–1835.

[33] K.L. Scrivener, W. Wieker, Advances in hydration of cements at low, ambient and elevated temperatures, Proceedings of the 8th International Congress on the Chemistry of Cement, New Delhi, India, 1992, pp. 447–482.

[34] P. Myers, Calcium aluminate cements—hydration of calcium aluminate cements, CERAM Research Ltd publication, 2007 full text at: http://www.azom.com/details.asp?ArticleID=1646.

[35] J.F. Mac Dowell, T. Huang, A. Chowdhury, Evaluation of stratlingite–hydrogarnet glass cement as a quick-setting patching mineral, Strategic highway research program, National Research Council, Amy Gray Light publisher, Washington, USA, 1992.

[36] V. Baroghel-Bouny, Caractérisation des pâtes de ciment et des bétons: méthodes, analyses, interprétations, Editions LCPC (Eds), Paris, France, 1994.

[37] C.A. Love, I.G. Richardson, A.R. Brough, Composition and structure C-S-H in white Portland cement-20% metakaolin paste hydrated at 25 °C, Cement and Concrete Research 37 (2) (2007) 109–117.

[38] S.Y. Hong, F.P. Glasser, Alkali sorption by C-S-H and C-A-S-H gels, Part II. Role of alumina, Cement and Concrete Research 32 (2002) 1101–1111.

[39] D.M.R. Brew, F.P. Glasser, The magnesia–silica gel phase in slag cements: alkali (K, Cs) sorption potential of synthetic gels, Cement and Concrete Research 35 (2005) 77–83.

[40] I.G. Richardson, The nature of the hydration products in hardened cement pastes, Cement & Concrete Composites 22 (2000) 97–113.

Glossary

Θ: Diffraction angle,
dTG(%)/dt: derived value of TG(%) with respect to time t,
T: Temperature,
Ti: Temperature *i*,
a_0: Amplitude of the peak,
a_1: Centre of the peak,
a_2: Width (>0) of the peak,
q_{CSH}: Amount of CSH,
q_{CH}: Amount of CH,
T_d: Temperature of decomposition,
C: molar content of CaO,
S: molar content of SiO2,
C/S: molar CaO/SiO_2 ratio,
$n\ Ca(OH)_2$: molar quantity of portlandite,
Bi: Binder i,
Pi: Paste i,
OPC: Ordinary Portland cement,
CEMI: Portland cement according to European standard EN 197-1,
CEMII: Portland slag cement (in this study) according to European standard EN 197-1,
GGBS: Blast furnace slag,
MK: Metakaolin,
A: Alite (C_3S),
B: Belite (C_2S),
C: Celite (C_3A),
E: Ettringite,
Q: Quartz,
C-A-H: Calcium aluminate hydrated,
C-A-S-H: Calcium aluminium silicate hydrate,
C_2ASH_8: Hydrated gehlenite.
C_3ASH_6: Hydrogarnet,
C_4AH_{13}: Hydrated calcium aluminate,
CH: Portlandite,
C-S-H: Gel of calcium silicate hydrate,
DTA: Differential analysis.
TGA: Thermal gravimetric analysis,
XRD: X-ray diffraction.